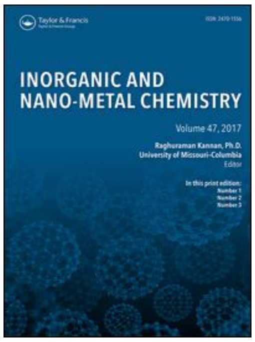

Inorganic and Nano-Metal Chemistry

ISSN: 2470-1556 (Print) 2470-1564 (Online) Journal homepage: http://www.tandfonline.com/loi/lsrt21

A new heterometallic coordination polymer: Synthesis, structure, and catalytic property

Qi-Feng Liu, Wei Liu, Yi-Po Cao, Yan-Li Dong & Hui-Min Liu

To cite this article: Qi-Feng Liu, Wei Liu, Yi-Po Cao, Yan-Li Dong & Hui-Min Liu (2017) A new heterometallic coordination polymer: Synthesis, structure, and catalytic property, Inorganic and Nano-Metal Chemistry, 47:1, 153-157, DOI: 10.1080/15533174.2016.1158188

To link to this article: http://dx.doi.org/10.1080/15533174.2016.1158188

INORGANIC AND NANO-METAL CHEMISTRY
2017, VOL. 47, NO. 1, 153–157
http://dx.doi.org/10.1080/15533174.2016.1158188

Taylor & Francis
Taylor & Francis Group

A new heterometallic coordination polymer: Synthesis, structure, and catalytic property

Qi-Feng Liu[a], Wei Liu[b], Yi-Po Cao[c], Yan-Li Dong[a], and Hui-Min Liu[a]

[a]College of Sciences, Agricultural University of Hebei, Baoding, P. R. China; [b]Department of Basic Medcine, logistics University of CAPF, Tianjin, P. R. China; [c]Tianjin Provincal Corps Hospital of Chinese People's Armed Police Force, Tianjin, P. R. China

ABSTRACT

A new heterometallic-organic framework, namely $[CuCa(tdc)_2(DMF)]_n$ (1 H_2tdc = 2,5-thiophenedicarboxylic acid, DMF = N,N′-dimethylformamide), has been successfully obtained through the solvothermal reactions of $CuCl_2$, $Ca(NO_3)_2$, and H_2tdc. Single-crystal structural analysis reveals that compound **1** features a 3D framework with the **irl** topology. Compound **1** has potential unsaturated metal sites after the removal of the coordinated DMF molecules, so it exhibits excellent catalytic activity for the diethylzinc addition to benzaldehyde.

ARTICLE HISTORY
Received 28 December 2015
Accepted 21 February 2016

KEYWORDS
Catalytic property; heterometallic compound; solvothermal reaction; topology

Introduction

Metal-organic frameworks (MOFs) have attracted much attention of scientists, owing to not only their impressive structural diversity but also their potential applications as functional materials in the fields of luminescence, gas storage/separation, magnetism, and heterogeneous catalysis.[1–5] Because the well-known HKUST-1 and MIL-101 have been successfully applied to catalyze the cyanosilylation of benzaldehyde,[6,7] MOF-based catalysis has become a research hotspot in recent years. According to previously reported documents, MOFs materials as catalysts must have accessible active metal centers in the structures.[8,9] Therefore, how to construct MOFs with appropriate active metal centers is extremely important. An effective method is to construct inorganic building blocks with terminal coordinated solvent molecules, the removal of which will generate coordinatively unsaturated metal sites. Although a lot of MOFs have been successfully applied to catalyze organic reactions, most of them are mainly single metal–based MOFs.[10–12] Comparatively speaking, heterometallic-organic frameworks as heterogeneous catalysts are rarely reported.[13,14] Based on these considerations, we successfully constructed a new heterometallic-organic framework, namely $[CuCa(tdc)_2(DMF)_2]_n$ (**1** H_2tdc = 2,5-thiophenedicarboxylic acid, DMF = N,N′-dimethylformamide). In this work, we will report the synthesis, structure, and catalytic property of this compound.

Experimental

Materials and methods

All chemicals were purchased commercially and used without further purification. X-ray intensities were collected on Oxford Xcalibur E diffractometer with graphite-monochromated Mo-*Kα* radiation ($\lambda = 0.71073$ Å). Elemental analyses (C, H, and N) were performed on an EA1110 CHNS-0 CE Elemental Analyzer. Powder X-ray diffraction (PXRD) analyses were recorded on a Rigaku Dmax2500 diffractometer with Cu-*Kα* radiation ($\lambda = 1.54056$ Å) with a step size of 0.05°. Thermogravimetric analyses were carried out on a NetzschSTA499C integration thermal analyzer under a nitrogen atmosphere from 30 to 800°C at a heating rate of 10°C/min.

Synthesis of $[CuCa(tdc)_2(DMF)_2]_n$

A mixture of $CuCl_2 \bullet 2H_2O$ (0.018 g, 0.1 mmol), $Ca(NO_3)_2 \bullet 4H_2O$ (0.024 g, 0.1 mmol), H_2tdc (0.034 g, 0.2 mmol), DMF (2 mL), and CH_3OH (2 mL) was placed in a 20 mL small vial. Then the mixture was heated to 70°C. The temperature was held for 60 h, then the vessel was cooled to room temperature over 30 min, leading to the formation of green crystals of **1** (yield: 35% based on H_2tdc). Anal. Calcd. for **1**, $C_{18}H_{16}N_2O_{10}S_2CuCa$: C, 36.73; H, 2.72; N, 4.76%. Found: C, 36.73; H, 2.74, N, 4.73%. IR (cm^{-1}): 3421(w), 1715(m), 1678(s), 1584(m), 1479(m), 1382 (m), 1373(m), 1109(w), 1021(w), 957(m), 892(m), 815(m), 778(w), 690(w).

X-ray crystallography

The X-ray single crystal structure analysis of **1** was performed on an Oxford Xcalibur E diffractometer (Mo-*Kα* radiation, $\lambda = 0.71073$ Å, graphite monochromator) at 293

CONTACT Hui-Min Liu ✉ huimin_liu3157@126.com College of Sciences, Agricultural University of Hebei, Baoding 071001, P. R. China.

Color versions of one or more of the figures in the article can be found online at www.tandfonline.com/lsrt.

CCDC No. 991738 contains the supplementary crystallographic data for this paper. These data can be obtained free of charge via www.ccdc.cam.ac.uk/data_request/cif, by emailing data_request@ccdc.cam.ac.uk, or by contacting The Cambridge Crystallographic Data Centre, 12, Union Road, Cambridge CB2 1EZ, UK. Fax:C44 1223336033.

Table 1. Crystallographic data for compound **1**.

Empirical formula	$C_{18}H_{16}N_2O_{10}S_2CaCu$
Temperature (K)	293(2)
Crystal color	green
Crystal size	0.18× 0.16× 0.14 mm^3
Formula weight	588.10
Crystal system	triclinic
Space group	$P-1$
a (Å)	10.3660(6)
b (Å)	10.4724(6)
c (Å)	12.9582(5)
α (°)	95.243(4)
β (°)	102.189(4)
γ (°)	106.434(5)
Volume (Å^3)	1301.57(12)
Z	2
Density (calcd.)	1.501 g/cm^3
Abs. coeff. (mm^{-1})	1.247
F(000)	598
Refinement method	Full-matrix least-squares on F^2
Reflections collections	10564
Independent reflections	5876 ($R_{\text{int}} = 0.0262$)
θ range for data collection	2.41–29.14
h,k,l range	$-32 \leq h \leq 18$, $-8 \leq k \leq 13$, $-17 \leq l \leq 17$
Goodness-of-fit on F^2	1.032
Final R indices [I>2sigma(I2)]	$R = 0.0453$, $wR_2 = 0.1196$
R (all data)	$R = 0.0591$, $wR_2 = 0.1297$
Largest difference peak and hole	0.906 and -0.647 Å^3

(2) K. Empirical absorption corrections were applied to the data using the SADABS program.[15] The structure was solved by the direct method and refined by the full-matrix least squares on F^2 using the SHELXL-97 program.[16] All of the non-hydrogen atoms were refined anisotropically, and the hydrogen atoms attached to carbon were located at their ideal positions. Experimental details for the structure determination are presented in Table 1. Selected bond lengths and angles are listed in Table 2.

Table 2. Selected bond lengths (Å) and angles (°) of compound **1**.

Cu(1)-O(3)^a	1.932(2)	Cu(1)-O(8)^b	1.946(2)
Cu(1)-O(1)	1.953(2)	Cu(1)-O(5)	2.001(2)
Ca(1)-O(7)^b	2.282(2)	Ca(1)-O(7)^c	2.282(2)
Ca(1)-O(2)	2.301(2)	Ca(1)-O(2)^d	2.301(2)
Ca(1)-O(10)^d	2.367(3)	Ca(1)-O(10)	2.367(3)
Ca(2)-O(4)^e	2.308(2)	Ca(2)-O(4)^a	2.308(2)
Ca(2)-O(6)	2.315(2)	Ca(2)-O(6)^f	2.315(2)
Ca(2)-O(9)	2.323(3)	Ca(2)-O(9)^f	2.323(3)
O(3)^a-Cu(1)-O(8)^b	90.48(10)	O(3)^a-Cu(1)-O(1)	165.00(10)
O(8)^b-Cu(1)-O(1)	92.68(11)	O(3)^a-Cu(1)-O(5)	92.28(11)
O(8)^b-Cu(1)-O(5)	169.39(10)	O(1)-Cu(1)-O(5)	87.29(11)
O(7)^b-Ca(1)-O(7)^c	180.000(1)	O(7)^b-Ca(1)-O(2)	86.99(9)
O(7)^c-Ca(1)-O(2)	93.01(9)	O(7)^b-Ca(1)-O(2)^d	93.01(9)
O(7)^c-Ca(1)-O(2)^d	86.99(9)	O(2)-Ca(1)-O(2)^d	180.00(11)
O(7)^b-Ca(1)-O(10)^d	95.07(12)	O(7)^c-Ca(1)-O(10)^d	84.93(12)
O(2)-Ca(1)-O(10)^d	88.35(11)	O(2)^d-Ca(1)-O(10)^d	91.65(11)
O(7)^b-Ca(1)-O(10)	84.93(12)	O(7)^c-Ca(1)-O(10)	95.07(12)
O(2)-Ca(1)-O(10)	91.65(11)	O(2)^d-Ca(1)-O(10)	88.35(11)
O(10)^d-Ca(1)-O(10)	180.00(13)	O(4)^e-Ca(2)-O(4)^a	180.00(14)
O(4)^e-Ca(2)-O(6)	92.19(8)	O(4)^a-Ca(2)-O(6)	87.81(8)
O(4)^e-Ca(2)-O(6)^f	87.81(8)	O(4)^a-Ca(2)-O(6)^f	92.19(8)
O(6)-Ca(2)-O(6)^f	180.00(14)	O(4)^e-Ca(2)-O(9)	91.03(12)
O(4)^a-Ca(2)-O(9)	88.97(12)	O(6)-Ca(2)-O(9)	89.73(10)
O(6)^f-Ca(2)-O(9)	90.27(10)	O(4)^e-Ca(2)-O(9)^f	88.97(12)
O(4)^a-Ca(2)-O(9)^f	91.03(12)	O(6)-Ca(2)-O(9)^f	90.27(10)
O(6)^f-Ca(2)-O(9)^f	89.73(10)	O(9)-Ca(2)-O(9)^f	180.00(15)

Symmetry codes: (a) $x-1, y, z$; (b) $x, y+1, z$; (c) $-x+2, -y, -z+1$; (d) $-x+2, -y+1, -z+1$; (e) $-x+2, -y, -z$; (f) $-x+1, -y, -z$.

Result and discussion

Description of the structure

Single crystal X-ray structural analysis reveals that compound **1** crystallizes in triclinic $P-1$ space group with the asymmetric unit containing one Cu(II) ion, two Ca(II) ions with the occupancy of 0.5, two tdc^{2-} ligands, and two coordinated DMF molecules. As shown in Figure 1, Cu1 is coordinated by four carboxylate oxygen atoms from four different tdc^{2-} ligands, displaying a quadrilateral geometric configuration. Ca1 and Ca2 are six-coordinated with octahedral coordination geometries, which are defined by four carboxylate oxygen atoms from four different tdc^{2-} ligands and two oxygen atoms of coordinated DMF molecules. The Cu-O and Ca-O distances are in the range of 1.932(2)–2.001(2) Å and 2.282(2)–2.367(2) Å, respectively. In **1**, tdc^{2-} ligand links four metal ions (two Ca(II) ions and two Cu(II) ions) with its two carboxylate groups in uniform bis-monodentate mode. The Cu(II) ions and Ca(II) ions are alternately linked by the carboxylate groups into a infinite chain subunit (Figure 2a). Each infinite chain is further connected to four adjacent infinite chains by tdc^{2-} ligands, resulting in the formation of the 3D framework (Figure 2c). To better understand this complicated framework of **1**, topological analysis based on nomenclature of rod packing was used to simplify this framework. The carboxylate C atoms are at the vertices of each infinite chain, and the connectivity between these C atoms results in a 1D zigzag ladder-like chain (Figure 2a). If the tdc^{2-} ligands can be reduced into rod-shaped linkers (Figure 2b), these zigzag ladder-like chains are further linked together by the rod-shaped linker, giving rise to a 3D network with **irl** topology (Figure 2d). As we known, heterometallic frameworks with **irl** topology are rarely reported.

Catalytic property

In compound **1**, each Ca(II) ion has two coordinated DMF molecules, and the coordinated DMF molecules can be removed out by the means of heating. The desolvated samples

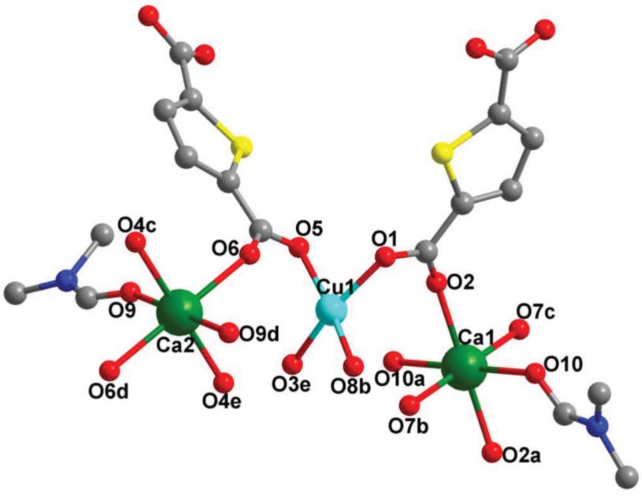

Figure 1. View of the coordination environments of Cu(II) and Ca(II) ions in **1**. Symmetry codes: (a) $2-x, 1-y, 1-z$; (b) $x, 1+y, z$; (c) $2-x, -y, 1-z$; (d) $1-x, -y, -z$; (e) $-1+x, y, z$.

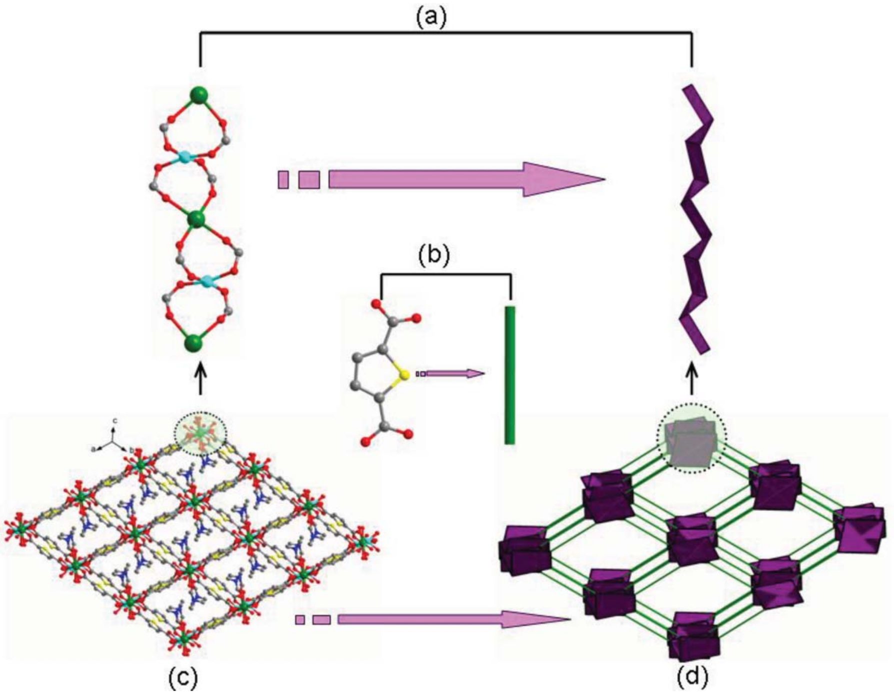

Figure 2. (a) 1D heterometallic chain subunit (left) and a zigzag ladder deduced from the connectivity between carboxylate C atoms. (b) Representation of tdc^{2-} ligand as linker. (c) The 3D framework of **1**. (d) Schematic representation of **irl** topological network for **1**.

have coordinately unsaturated metal sites, so it can act as Lewis acid catalyst. To evaluate the catalytic activity of the desolvated sample of **1**, the reaction of diethylzinc addition to benzaldehyde was used (Figure 3a). First, compound **1** was dried under vacuum at 250°C for 2 h, affording the activated samples suitable for the catalytic reaction. Second, the activated samples were placed in a 25 mL Schlenk flask and then vacuumized for 10 min. Third, the hexane (2 mL) solvent was added *via* syringe under nitrogen and the mixture was stirred for 30 min. Fourth, benzaldehyde (0.25 mL) and diethylzinc (in n-hexane, 1 mL) were added, and the new mixture was stirred under nitrogen at 25°C. In order to detect the yield of the phenylpropanol, a small amount of solution was taken out in a certain time interval and quenched with saturated NH_4Cl solution and ethyl acetate. The composition of the reaction mixture was characterized by the gas chromatograph (GC) analysis (Figure 4). From the GC, we can observe the phenylpropanol in the products. At the time of 30 h, the concentration of phenylpropanol reached 47.8%. After 30 h, the concentration of phenylpropanol has no obvious change (Figure 3b). In addition, we have also done several

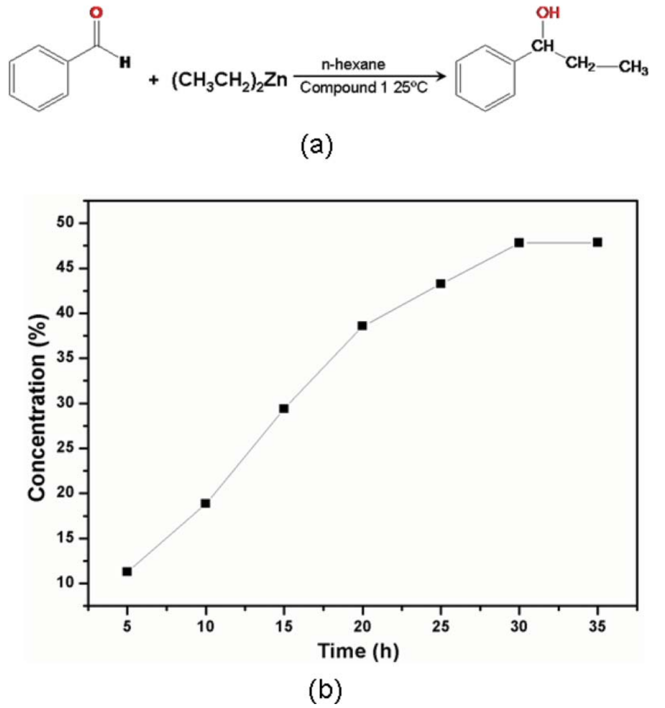

Figure 3. (a) The addition reactions of diethylzinc with benzaldehyde. (b) The concentration of phenylpropanol with time for **1**.

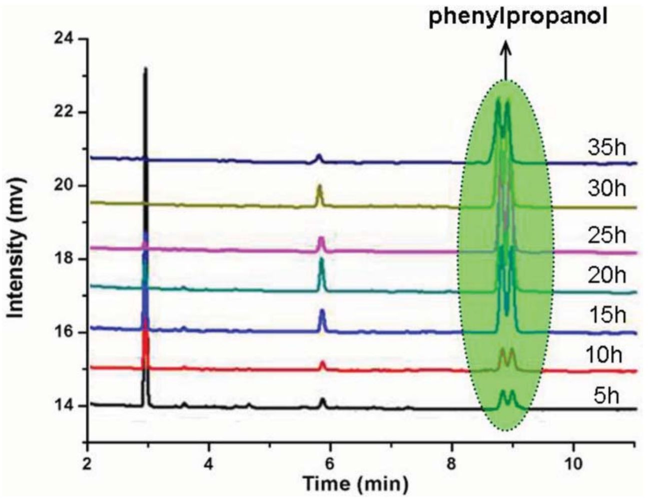

Figure 4. The view of the gas chromatograph spectrum for compound 1 as the catalyst.

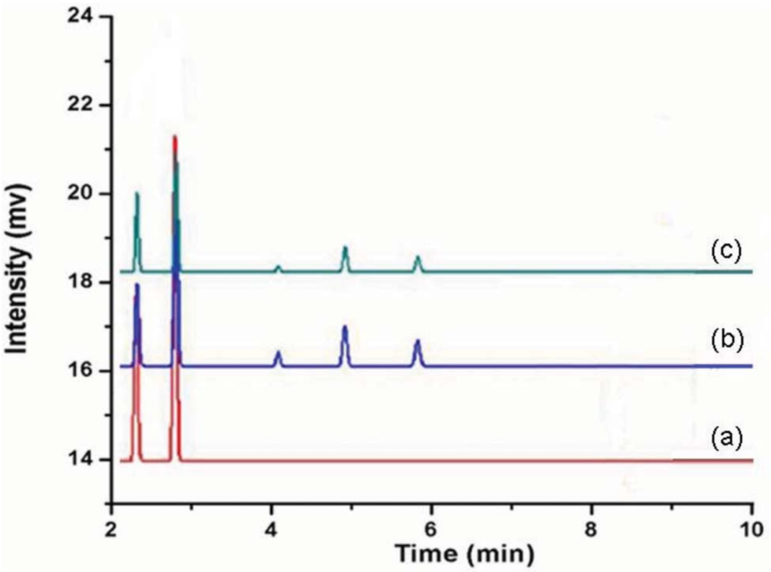

Figure 5. The view of the gas chromatograph spectrum. (a) Metal salts alone. (b) Free organic ligand. (c) Metal salts and free organic ligand.

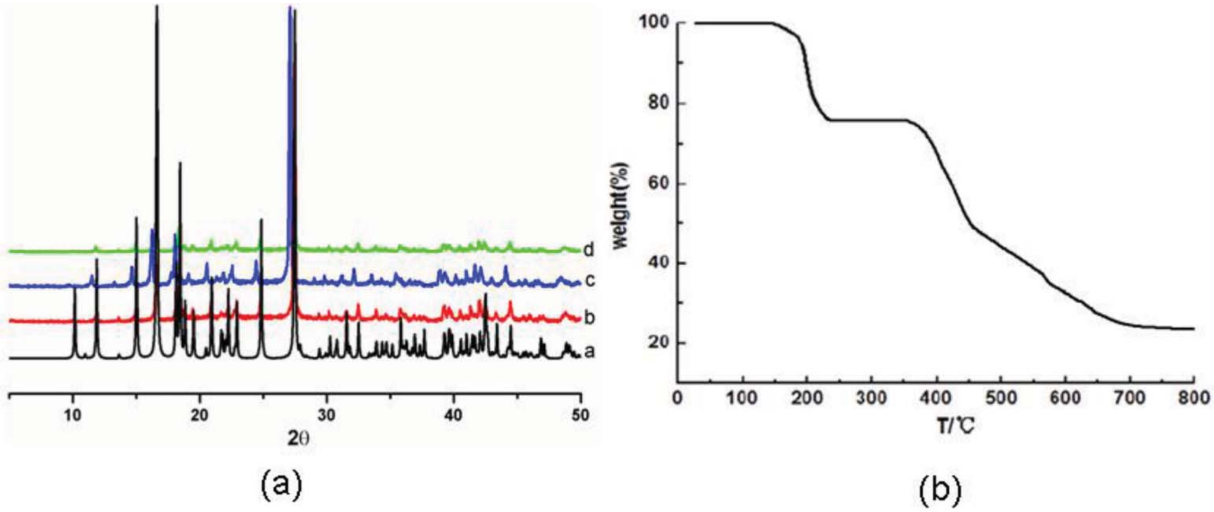

Figure 6. (a) Powder X-ray diffraction patterns for 1 (a, simulated powder patterns; b, sample powder patterns; c, thermal tread sample patterns [250°C for 2 h]; d, after catalytic experiment). (b) TG curve of 1.

parallel experiments by using the metal salts, organic ligand as well as the mixture of organic ligand and metal salts under the similar reaction conditions, the results suggest that they show no catalytic effect for this reaction (Figure 5).

PXRD patterns and thermal analysis

The phase purity of compound **1** was confirmed by the powder X-ray diffraction. The experimental pattern of the bulk samples of **1** is in good agreement with the simulated one based on the single-crystal diffraction data. The peak of powder X-ray pattern for the activated sample moved a little to the lower angle, indicating that the desolvated sample may have a little change. The powder X-ray pattern of the activated sample after catalysis is consistent with that of the activated samples (Figure 6). Thermal analysis for **1** was also performed on polycrystalline samples under N_2 atmosphere in the temperature range of 30–800°C. As shown in Figure 6b, the weight loss of about 24.32% (calcd. 24.49%) in the temperature range of 150–234°C corresponds to the release of the coordinated DMF molecules. Then, the desolvated samples can be stable up to 310°C. After 310°C, a sharp weight loss may be assigned to the decomposition of the organic ligand.

Conclusions

In summary, we have successfully obtained a new 3D heterometallic-organic framework with **irl** topology, which has potential unsaturated sites after the removal of the coordinated DMF molecules. It shows good catalytic activity for the diethylzinc addition to benzaldehyde.

Funding

This work was supported by grants from the Sci-technical Support Project of Hebei Province (14227115D).

References

1. Yaghi, O. M.; O'Keeffe, M.; Ockwig, N. W.; Chae, H. K.; Eddaoudi, M.; Kim, J. Reticular synthesis and the design of new materials. *Nature* **2003**, *423*, 705–714.
2. Chen, B. L.; Xiang, S. G.; Qian, G. D. Metal—organic frameworks with functional pores for recognition of small molecules. *Acc. Chem. Res.* **2010**, *43*, 1115–1124.
3. Zhou, H. C.; Long, J. R.; Yaghi, O. M. Introduction to metal-organic frameworks. *Chem. Rev.* **2012**, *112*, 673–674.
4. Zhang, H. X.; Wang, F.; Tan, Y. X.; Kang, Y.; Zhang, J. Homochiral porous metal-organic frameworks containing only achiral building blocks for enantioselective separation. *J. Mater. Chem.* **2012**, *22* 16288–16292.
5. Horcajada, P.; Gref, R.; Baati, T.; Allan, P. K.; Maurin, G.; Couvreur, P.; Morris, R. E.; Serre, C. Metal–Organic frameworks in biomedicine. *Chem. Rev.* **2012**, *112*, 1232–1268.
6. Kang, Y.; Nickerl, G.; Henschel, A.; Grünker, R.; Gedrich, K.; Kaskel, S. Chiral metal–organic frameworks and their application in asymmetric catalysis and stereoselective separation. *Chem. Eng. Technol.* **2011**, *83*, 90–103.
7. Schlichte, K.; Kratzke, T.; Kaskel, S. Improved synthesis, thermal stability and catalytic properties of the metal-organic framework compound $Cu_3(BTC)_2$. *Microporous Mesoporous Mater.* **2004**, *73*, 81–88.
8. Wang, Z.; Chen, G.; Ding, K. Self-supported catalysts. *Chem. Rev.* **2009**, *109*, 322–359.
9. Henschel, A.; Gedrich, K.; Kraehnert, R.; Kaskel, S. Catalytic properties of MIL-101. *Chem. Commun.* **2008**, 4192–4194.
10. Ma, L.; Wu, C. D.; Wanderley, M. M.; Lin, W. B. Single-crystal to single-crystal cross-linking of an interpenetrating chiral metal–organic framework and implications in asymmetric catalysis. *Angew. Chem. Int. Ed.* **2010**, *49*, 8244–8248.
11. Wu, C. D.; Lin, W. B. Heterogeneous asymmetric catalysis with homochiral metal–organic frameworks: network-structure-dependent catalytic activity. *Angew. Chem. Int. Ed.* **2007**, *46*, 119, 1075–1078.
12. Chen, Y. F.; Ma, Y. C.; Chen, S. M. A chiral tetrahedral framework with tetrahedral guests for catalysis and photoluminescence. *Cryst. Growth Des.* **2013**, *13*, 4154–4157.
13. Chen, Y. F.; Ma, Y. C.; Zhang, H. B.; Chen, S. M. An effective approach for constructing acentric heterometallic-organic framework with catalytic activity. *Inorg. Chem. Comm.* **2014**, *43*, 27–30.
14. Tan, Y. X.; He, Y. P.; Zhang, J. Cluster-organic framework materials as heterogeneous catalysts for high efficient addition reaction of diethylzinc to aromatic aldehydes. *Chem. Mater.* **2012**, *24*, 4711–4716.
15. Sheldrick, G. M. *SADABS*; University of Göttingen: Göttingen, Germany, **1996**.
16. Sheldrick, G. M. *SHELXTL-97: Program for Refining Crystal Structure Refinement*; University of Göttingen, Germany, **1997**.